

A Highly Efficient Wide-Angle Symmetric Meta-Absorber in Visible to Near-Infrared

Md Raihan

Dept. of EEE

International Islamic

University Chittagong

Chattogram, Bangladesh

mohammedraihan133@gmail.com

S. E. A. Himu

Dept. of EME

Nagoya Institute

of Technology

Nagoya, Japan

erfanhimu@gmail.com

Kazi Mohammed Abdullah

Dept. of ETE

International Islamic

University Chittagong

Chattogram, Bangladesh

kazitusher636@gmail.com

Md Shahazan Parves

Dept. of EEE

International Islamic

University Chittagong

Chattogram, Bangladesh

parveziuc4708@gmail.com

Tasneem Tabassum

Dept. of EEE

International Islamic

University Chittagong

Chattogram, Bangladesh

oyshi.tasneem2002@gmail.com

Kazi Ashaduzzaman

Dept. of EEE

International Islamic

University Chittagong

Chattogram, Bangladesh

kaziashad12@gmail.com

Arafat Ibne Ikram

Dept. of EEE

International Islamic

University Chittagong

Chattogram, Bangladesh

arafatibne.ikram@gmail.com

Abstract—Absorber working in optical wavelength draws significant attraction due to its vast field of application. A high-efficiency metamaterial absorber (MMA) is proposed in this study to utilize solar radiation perfectly. The MMA achieves 97.5% of total average absorption for the wavelength 375 nm to 1000 nm. From 375 to 700 nm (visible band) it achieves 97.47% average absorption. This symmetrical meta-structure is polarization insensitive along with the independence of angular sensitivity up to 70°. Recent developments are discussed on the attainment of several desired absorber characteristics, including flexibility, tunability, polarization and angle independence, and broadband and multiband operation. Additionally, recommendations for future lines of inquiry are provided.

Keywords—MMA, CST, absorber, solar harvesting, polarization, visible region, absorption

I. INTRODUCTION

Research on electromagnetic wave utilization focuses on meta-materials (MTM's) an artificially engineered material designed to surpass natural substance properties. The term "meta-material" signifies intentional deviation from natural material characteristics. These synthetics exhibit exceptional properties, diverging from typical natural material traits. Precisely engineering the design and structure of meta-materials MTM's at a sub-wavelength scale allows the attainment of negative permeability [?], [1], negative permittivity [2], and negative refractive index [3] which are distinctive properties not found in natural materials [4].

These distinctive characteristics make the material applicable across a broad range of disciplines including sensing, energy harvesting [5], telecommunication [6], satellite application [7], imaging system [8], super lenses [9], and wireless application [10]. Meta-material absorbers are created to soak up electromagnetic waves that come in, covering a broad [11],

[12] spectrum or particular frequencies [13], [14]. Research has explored the efficiency of meta-material absorbers in absorbing electromagnetic waves across the spectrum, from microwaves to optical wavelengths [15]. In 2008 Landy et al. [16] proposed the first MMA (meta-material absorber), which offered the advantages of thin thickness and compact size compared to conventional absorbers. Subsequent research efforts delved into exploring potential applications and optimizing the outcomes. Numerous studies have been proposed for various frequency ranges such as terahertz [17], [18], gigahertz [19], visible [20], and infrared [21] frequencies. MTM's find diverse applications, such as capturing wasted heat, detecting multiple infrared colors, and achieving cooling below ambient temperature. Studies in sensing, thermal imaging, and energy trapping have been proposed in these domains. Notably, absorbers in the visible spectrum are significant, covering 48% of solar wavelengths [22]. Solar energy conversion is one very promising use for meta-material absorbers in the visible spectrum. For many energy-related applications, especially in the field of solar energy harvesting, complete absorption of visible light is essential [23].

Researchers have proposed several architectures for a meta-material absorber that include one or more layers of metal-dielectric metal. These designs demonstrate effective absorption efficacy across a wide range of wavelengths and angles and are independent of polarization in the visible region. Luo et al. [24] proposed an absorber that operates in the visible region (400 nm to 700 nm) that achieved 80% average absorption for a wide angle up to 60°. An absorber operating in the range of 400 nm to 700 nm exhibited an absorption rate of 80%, as reported in a study by P. Zhu et al. [25] This absorber is composed of stacked layers of Cu/Si3N4/Cu. A three-layered absorber based on aluminum and silicon dioxide

demonstrated an absorptivity of 95%, spanning the wavelength range from 400 nm to 650 nm [26]. In a study suggested by M. Bagmanci et al. [27]–[29] 91% absorption capacity was attained in the frequency range 430 THz to 770 THz. Besides energy harvesting applications, absorbers operating in visible may find applications in various fields. Mahmud et al [30] designed an absorber with an average efficiency of 96.77%, operating in the wavelength range of 389.34 nm to 697.19 nm. This absorber holds potential applications in optical sensors and light detectors.

The mentioned works operate within the visible frequency range; however, this bandwidth covers only 48% of the sun’s total emission. Additionally, high absorption is required to demonstrate efficiency, along with polarization insensitivity and angular independence. To overcome the limitations of these recent works, we propose a noble MMA capable of achieving a high absorption of about 97.5% throughout the entire operational wavelength, with an average absorption of 95.47% in the visible region. The MMA obtained a broad 625 nm bandwidth. Additionally, the proposed absorber maintains its efficiency with polarization and angular independence up to 70°. Such a suggested MMA can be utilized in solar thermophotovoltaic (STPV) systems, enhancing solar cell efficiency, and thermal energy conversion systems.

II. STRUCTURE DESIGN

A common meta-absorber consists of a three-layer metal-dielectric-metal. The material in these layers plays an important role in absorption characteristics. Tungsten is an ideal material for solar electromagnetic harvesting due to its cost-effectiveness and exceptional chemical durability inhibits corrosion resulting from interactions with oxygen, acids, and alkalis [31], [32].

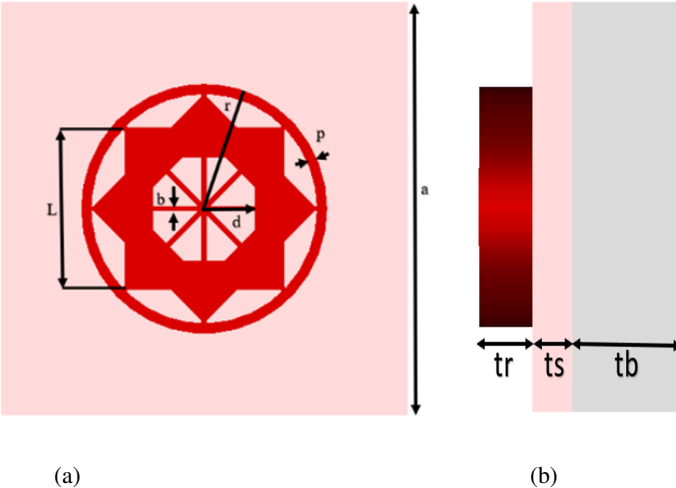


Fig. 1: Design evaluation (a) dimension in front view (b) thickness of layers

This characteristic allows for its use in robust environments. Additionally, tungsten boasts a significantly higher melting

point of approximately 3,422 °C. The suggested design comprises three layers composed of tungsten and silicon dioxide. The absorption formula is expressed as in EQ. (1),

$$A(\omega) = 1 - T(\omega) - R(\omega) \quad (1)$$

The recommended metasurface absorber design was developed through the utilization of advanced 3D electromagnetic analysis software, specifically CST MWS 2019. To accurately simulate and model electromagnetic phenomena, this software implements a robust combination of the Finite Difference Frequency Domain (FDFD) solver, the Finite Integration Technique (FIT), and a tetrahedral mesh component. For both the x and y-axes, unit cell boundary conditions were used. In both the positive and negative dimensions along the z-axis, the Floquet port was configured as an excitation source.

TABLE I: The parameter list of the absorber

Parameter	Value (nm)	Parameter	Value (nm)
a	400	r	120
b	5	tb	150
d	49.6	tr	75
L	155.55	ts	55

The absorption coefficient is determined by the combination of transmission ($T(\omega)$) and reflection ($R(\omega)$), where $T(\omega)$ and $R(\omega)$ represent transmission and reflection coefficients, respectively. In the case of the bottom layer made of tungsten, a metal material, it impedes the transmission of the incident wave, resulting in zero transmission. Consequently, perfect absorption is dependent on achieving zero reflection, given that absorption is the complementary factor to reflection. Thus EQ. (1), becomes,

$$A(\omega) = 1 - R(\omega) \quad (2)$$

Design evaluation and dimension in the front view with respective thickness of layers are shown in Fig 1. Various theories have been examined to comprehend the absorption mechanism of Metamaterial Absorbers (MMA). One such theory is the impedance matching theory. According to this concept, perfect or complete absorption takes place when the impedance of the MMA structure matches that of free space. Reflection in terms of impedance can be defined by, $R(\omega) = [(Z(\omega) - Z_0) - (Z(\omega) + Z_0)]^2$. We can express impedance in terms of permeability and permittivity $Z = \sqrt{(\mu/\epsilon)}$ [29]. Thus, the material property and the structural design influence the absorption behavior.

A. Angular and polarization insensitivity

As the proposed design operates in visible and NIR regions in which the radiation comes from the sun. to absorb properly the incoming radiation the absorber should be polarization and angular insensitive. To make polarization and angular insensitive structure should be symmetrical in every aspect of the viewing angle. Fig. 1 depicts the insensitivity of the polarization angle(ϕ) and incident angle(θ), where the suggested one is angle and polarization-independent in different modes (TE, TM, and TEM).

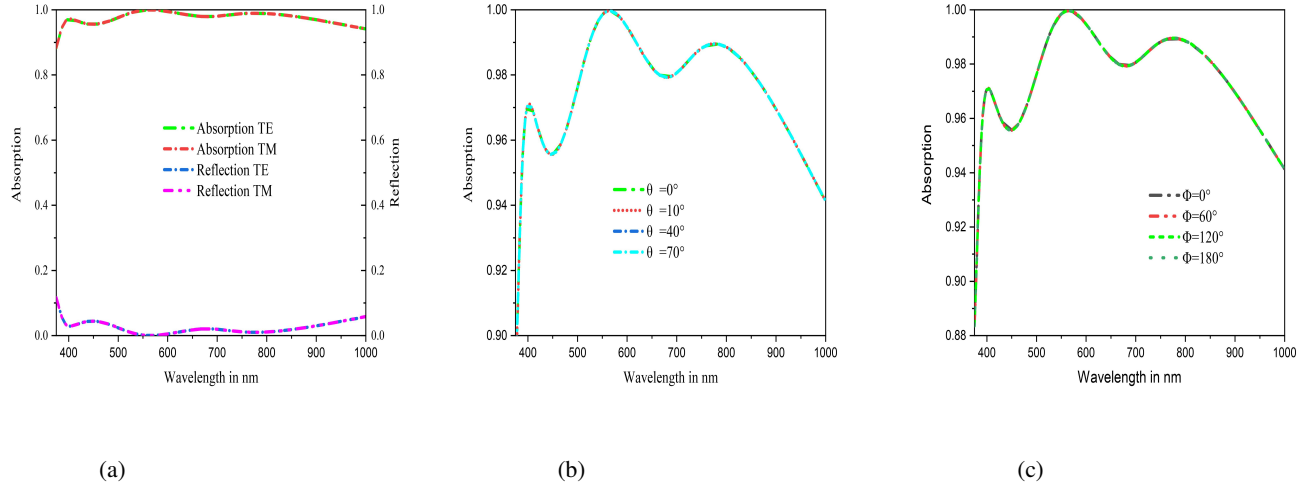


Fig. 2: Demonstration of absorption under (a) various propagation modes, (b) different incident angles (c) different polarization angle

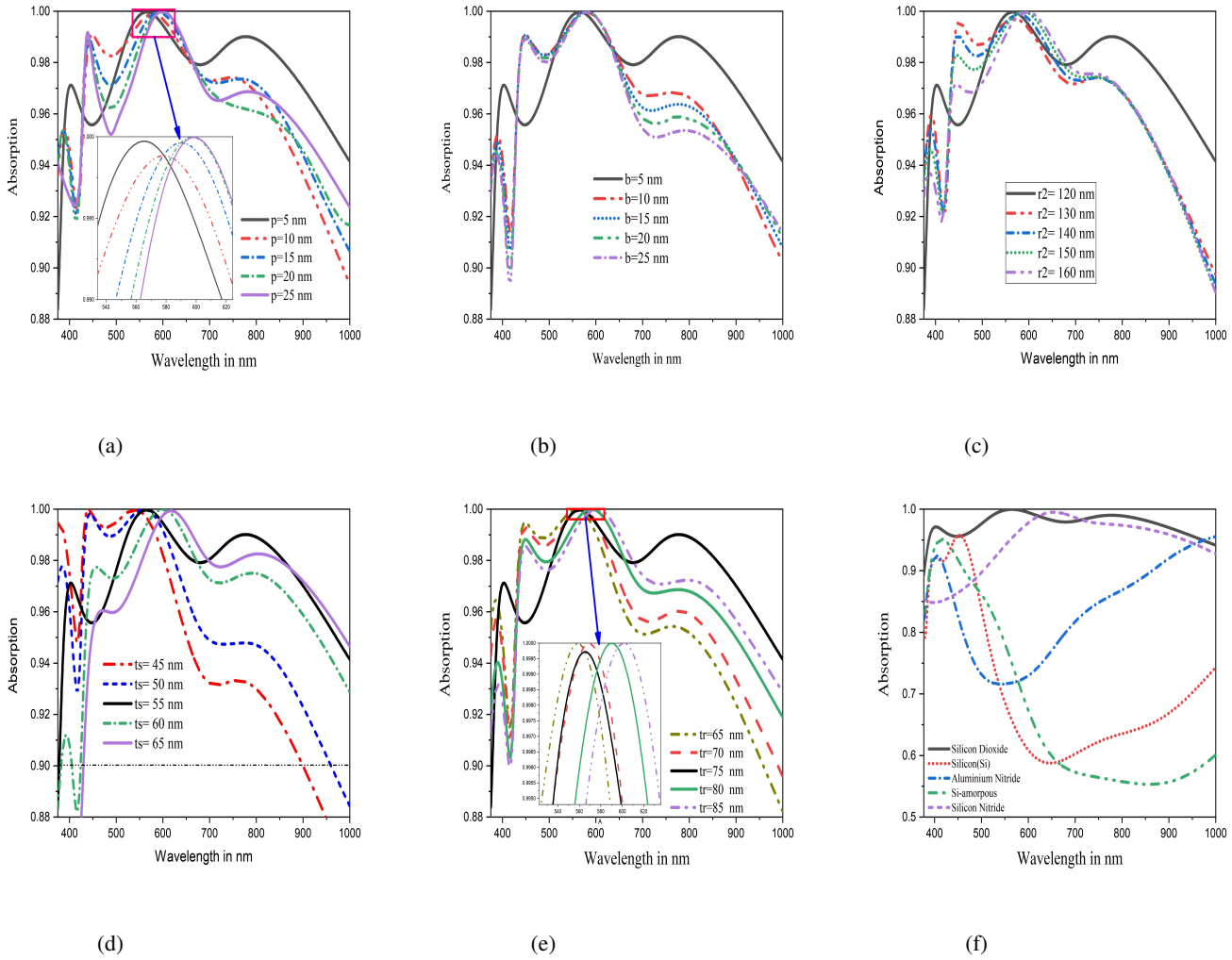


Fig. 3: Illustration of absorption for (a) changing parameter b (b) changing parameter p (c) changing parameter $r2$ (d) changing thickness t_s (e) changing thickness t_r (f) different dielectric material

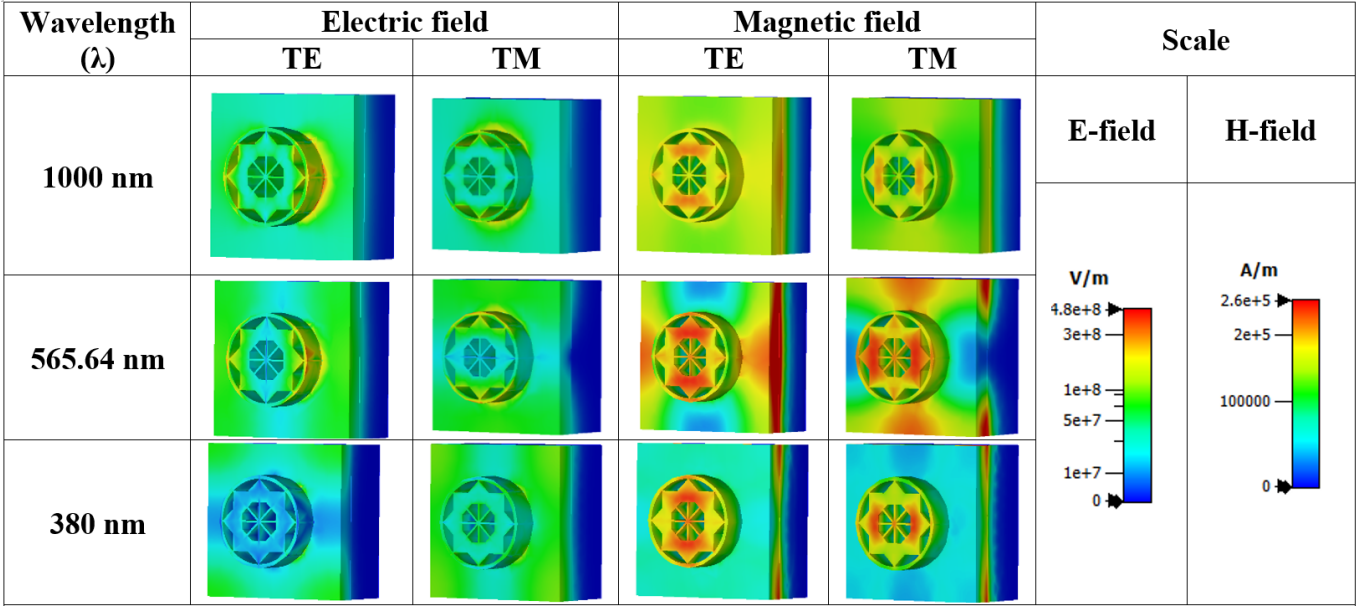


Fig. 4: E-field and H-field distribution of the MMA for TE and TM mode

B. Parametric sweep analysis

To achieve optimum output from the proposed design, a parametric sweep analysis was performed to select the optimized value for the structure. As in Table I various parameters have been mentioned. Fig. 2(a) and Fig. 2(b) depict the absorption property for changing the radius of the outer circle and the width of the circle. Maximum average absorption was found for the value $p=10$ nm which is 97.01%, 96.81%, 96.8%, 96.5%, 96.32% average found for the values 5,15,20,25 nm. Efficiency increases with the increase in width from 5 nm to 10 nm, and further increase reduces the efficiency.

Centre line width is denoted as ‘b’ which is also optimized by simulating the value from 5 nm to 25 nm. An average of 97% was found for this value and the rest of the achieved average absorption for testing values are 96.80%, 96.64%, 96.44%, and 96.24%. best absorption we achieved for the lowest value of width as we can see from the absorption value with an increase in width absorption drops. The radius of the outer circle also varied from 120 nm to 160 nm with an increment of 10 nm.

The most important parameters are the thickness of dielectric ‘ts’ and resonator ‘tr’. Dielectric thickness changed from 45 nm to 55 nm with an increase of 5 nm. 96.44%, 96.77%, 97.5%, 96.02%, and 95% average efficiency was found for the thicknesses of 45 nm, 50 nm, 55 nm, 60 nm, and 65 nm respectively. Thickness ‘ts’ = 55 nm suit best for the design best as it matched the free space impedance. In terms of resonator thickness change 96.5%, 96.68%, 97.5%, 96.65%, and 96.6% average were achieved for the thickness values 65 nm 70 nm 75 nm 80 nm, and 85 nm respectively. In Fig. 3 demonstration of the influence of structure parameters on absorption is given. Fig. 3(f) absorption under various substrate materials also investigates where silicon dioxide

achieved excellent absorption. MMA with a-silicon, silicon, and silicon nitride can be used as a half absorber [33].

The electric field and magnetic given in Fig 4 where we can see that the magnetic field is confined mostly on the resonator whereas the electric field is mostly distributed on the substrate. The wavelength of the incident wave absorbs properly as the capacitance is created by the resonator and dielectric layer.

III. COMPARISON

From the previous literature review and prior work, it is found that a wideband MMA with excellent absorption above 95% is still a concern of research. In addition, polarization and angular insensitivity are also a matter of concern for designing such an absorber. In Table II we can see that the proposed absorber is a great choice compared to other suggested work. To express the uniqueness and contribution of our work in Table II we have demonstrated similar works recently done by researchers. The efficiency of an absorber is often determined by its ultra-broadband capability, along with polarization and angular insensitivity. Table 2 reveals that the proposed absorber boasts remarkable attributes, including an ultra-broad absorption bandwidth of 625 nm and an outstanding average absorption rate of 97.5%. Furthermore, its angular and polarization insensitivity further enhance its superiority in every aspect. Therefore, compared to other works, it is evident that the proposed absorber stands out as an excellent choice.

IV. CONCLUSIONS

In this study, we introduced a broadband, highly efficient meta-material absorber. The absorber adopts a sandwich-type three-layer structure, achieving a remarkable absorption rate of 97.5% across the entire operational bandwidth. The meta-material absorber demonstrates angular insensitivity up to 70° and polarization independence. These characteristics make it

TABLE II: Comparison between previous work

Ref	Size	Layer	Material	Operation range	Bandwidth	Polarization and Angular insensitivity	Average absorption (%)
[30]	1000×1000×225	3	W, SiO ₂	400-700	308	Yes, $\theta \leq 60^\circ$	96.7
[34]	1000×1000×165	3	W, Quartz	380-750	375	Yes, $\theta \leq 45^\circ$	90
[35]	1555×1555×560	3	A-Si, Ag, ITO		380	Yes, $\theta \leq 45^\circ$	90.1
[35]	1000×1000×644	3	Au, SO ₂		380	Yes, $\theta \leq 80^\circ$	N/A
[11]	400×400×245	3	W, SiO ₂		459	Yes, $\theta \leq 60^\circ$	Above 90
[34]	1000×1000×165	3	W, Quartz		375	Yes, $\theta \leq 45^\circ$	90

well-suited for applications such as efficient thermal energy conversion systems, solar thermo-photovoltaic systems, and the enhancement of solar photovoltaic cell efficiency.

REFERENCES

- [1] R. Marqués, F. Medina, and R. Rafii-El-Idrissi, "Role of bianisotropy in negative permeability and left-handed metamaterials," *Physical Review B*, vol. 65, no. 14, p. 144440, 2002.
- [2] D. Schurig, J. Mock, and D. Smith, "Electric-field-coupled resonators for negative permittivity metamaterials," *Applied physics letters*, vol. 88, no. 4, 2006.
- [3] W. J. Padilla, D. N. Basov, and D. R. Smith, "Negative refractive index metamaterials," *Materials today*, vol. 9, no. 7-8, pp. 28–35, 2006.
- [4] A. Grigorenko, A. Geim, H. Gleeson, Y. Zhang, A. Firsov, I. Khrushchev, and J. Petrovic, "Nanofabricated media with negative permeability at visible frequencies," *Nature*, vol. 438, no. 7066, pp. 335–338, 2005.
- [5] Z.-Q. Lu, L. Zhao, H. Ding, and L.-Q. Chen, "A dual-functional metamaterial for integrated vibration isolation and energy harvesting," *Journal of Sound and Vibration*, vol. 509, p. 116251, 2021.
- [6] M. AbuHussain and U. C. Hasar, "Design of x-bandpass waveguide chebyshev filter based on csrr metamaterial for telecommunication systems," *Electronics*, vol. 9, no. 1, p. 101, 2020.
- [7] T. Alam, A. F. Almutairi, M. Samsuzzaman, M. Cho, and M. T. Islam, "Metamaterial array based meander line planar antenna for cube satellite communication," *Scientific reports*, vol. 11, no. 1, p. 14087, 2021.
- [8] W. J. Padilla and R. D. Averitt, "Imaging with metamaterials," *Nature Reviews Physics*, vol. 4, no. 2, pp. 85–100, 2022.
- [9] X. Zhang and Z. Liu, "Superlenses to overcome the diffraction limit," *Nature materials*, vol. 7, no. 6, pp. 435–441, 2008.
- [10] K. Jairath, N. Singh, M. Shabaz, V. Jagota, B. K. Singh *et al.*, "Performance analysis of metamaterial-inspired structure loaded antennas for narrow range wireless communication," *scientific programming*, vol. 2022, 2022.
- [11] C. Cao and Y. Cheng, "A broadband plasmonic light absorber based on a tungsten meander-ring-resonator in visible region," *Applied Physics A*, vol. 125, pp. 1–8, 2019.
- [12] R. Kumar, B. K. Singh, and P. C. Pandey, "Cone-shaped resonator-based highly efficient broadband polarization-independent metamaterial absorber for solar energy harvesting," *Research Square*, 2022.
- [13] Z. Yin, Y. Lu, S. Gao, J. Yang, W. Lai, Z. Li, and G. Deng, "Optically transparent and single-band metamaterial absorber based on indium-tin-oxide," *International Journal of RF and Microwave Computer-Aided Engineering*, vol. 29, no. 2, p. e21536, 2019.
- [14] S. E. A. Himu, S. Sultana, M. S. H. Chowdhury, A. I. Ikram, H. R. Saium, and M. M. Hossain, "Modification of dynamic logic circuit design technique for minimizing leakage current and propagation delay," in *2022 4th International Conference on Sustainable Technologies for Industry 4.0 (STI)*. IEEE, 2022, pp. 1–5.
- [15] R. Bilal, M. Saeed, P. Choudhury, M. Baqir, W. Kamal, M. M. Ali, and A. A. Rahim, "Elliptical metallic rings-shaped fractal metamaterial absorber in the visible regime," *Scientific reports*, vol. 10, no. 1, p. 14035, 2020.
- [16] N. I. Landy, S. Sajuyigbe, J. J. Mock, D. R. Smith, and W. J. Padilla, "Perfect metamaterial absorber," *Physical review letters*, vol. 100, no. 20, p. 207402, 2008.
- [17] P. Fu, F. Liu, G. J. Ren, F. Su, D. Li, and J. Q. Yao, "A broadband metamaterial absorber based on multi-layer graphene in the terahertz region," *Optics Communications*, vol. 417, pp. 62–66, 2018.
- [18] D. Hu, T. Meng, H. Wang, Y. Ma, and Q. Zhu, "Ultra-narrow-band terahertz perfect metamaterial absorber for refractive index sensing application," *Results in Physics*, vol. 19, p. 103567, 2020.
- [19] M. F. Zafar and U. Masud, "A multiple-bands metamaterial absorber based in x, ku and k-band," *Research Square*, 2021.
- [20] D. Shin, G. Kang, P. Gupta, S. Behera, H. Lee, A. M. Urbas, W. Park, and K. Kim, "Thermoplasmonic and photothermal metamaterials for solar energy applications," *Advanced Optical Materials*, vol. 6, no. 18, p. 1800317, 2018.
- [21] M. J. Hossain, M. R. I. Faruque, and M. T. Islam, "Perfect metamaterial absorber with high fractional bandwidth for solar energy harvesting," *PLoS One*, vol. 13, no. 11, p. e0207314, 2018.
- [22] S. K. Patel, S. Charola, and Parmar, "Broadband metasurface solar absorber in the visible and near-infrared region," *Materials Research Express*, vol. 6, no. 8, p. 086213, 2019.
- [23] R. Kumar, B. K. Singh, R. K. Tiwari, and P. C. Pandey, "Perfect selective metamaterial absorber with thin-film of gaas layer in the visible region for solar cell applications," *Optical and Quantum Electronics*, vol. 54, no. 7, p. 416, 2022.
- [24] M. Luo, S. Shen, L. Zhou, and Wu, "Broadband, wide-angle, and polarization-independent metamaterial absorber for the visible regime," *Optics express*, vol. 25, no. 14, pp. 16 715–16 724, 2017.
- [25] P. Zhu and L. Jay Guo, "High performance broadband absorber in the visible band by engineered dispersion and geometry of a metal-dielectric-metal stack," *Applied Physics Letters*, vol. 101, no. 24, 2012.
- [26] Y.-C. Lai, C.-Y. Chen, Y.-T. Hung, and C.-Y. Chen, "Extending absorption edge through the hybrid resonator-based absorber with wideband and near-perfect absorption in visible region," *Materials*, vol. 13, no. 6, p. 1470, 2020.
- [27] M. Bagmanci, M. Karaaslan, and C. Sabah, "Solar energy harvesting with ultra-broadband metamaterial absorber," *International journal of modern physics B*, vol. 33, no. 08, p. 1950056, 2019.
- [28] A. I. Ikram, M. Shafiqullah, M. R. Islam, and M. K. Rocky, "Techno-economic assessment and environmental impact analysis of hybrid storage system integrated microgrid," *Arabian Journal for Science and Engineering*, Feb 2024.
- [29] A. I. Ikram, A. Ullah, D. Datta, A. Islam, and T. Ahmed, "Optimizing energy consumption in smart homes: Load scheduling approaches," *IET Power Electronics*, 2024.
- [30] S. Mahmud, S. S. Islam, K. Mat, M. E. Chowdhury, H. Rmili, and M. T. Islam, "Design and parametric analysis of a wide-angle polarization-insensitive metamaterial absorber with a star shape resonator for optical wavelength applications," *Results in Physics*, vol. 18, p. 103259, 2020.
- [31] Y. Tian, X. Liu, F. Chen, and Y. Zheng, "Perfect grating-mie-metamaterial based spectrally selective solar absorbers," *OSA Continuum*, vol. 2, no. 11, pp. 3223–3239, 2019.
- [32] J. Li, X. Chen, Z. Yi, H. Yang, Y. Tang, Y. Yi, W. Yao, J. Wang, and Y. Yi, "Broadband solar energy absorber based on monolayer molybdenum disulfide using tungsten elliptical arrays," *Materials Today Energy*, vol. 16, p. 100390, 2020.
- [33] S. Mahmud, S. S. Islam, A. F. Almutairi, and M. T. Islam, "A wide incident angle, ultrathin, polarization-insensitive metamaterial absorber for optical wavelength applications," *Ieee Access*, vol. 8, pp. 129 525–129 541, 2020.
- [34] I. Hossain, M. Samsuzzaman, M. Moniruzzaman, B. B. Bais, M. S. J. Singh, and M. T. Islam, "Polarization-independent broadband optical regime metamaterial absorber for solar harvesting: A numerical approach," *Chinese Journal of Physics*, vol. 71, pp. 699–715, 2021.
- [35] J. Fang and B. Wang, "Optical capture capability enhancement by right-angled triangular visible absorber," *Physics Letters A*, vol. 404, p. 127404, 2021.